Efficient and Ultrafast Formation of Long-Lived Charge-Transfer Exciton State in Atomically Thin Cadmium Selenide/Cadmium Telluride Type-II Heteronanosheets

Kaifeng Wu,[†] Qiuyang Li,[†] Yanyan Jia,[‡] James R. McBride,[§] Zhao-xiong Xie,[‡] and Tianquan Lian*[,†]

[†]Department of Chemistry, Emory University, 1515 Dickey Drive, NE, Atlanta, Georgia 30322, United States, [‡]State Key Laboratory for Physical Chemistry of Solid Surfaces and Department of Chemistry, College of Chemistry and Chemical Engineering, Xiamen University, Xiamen 361005, China, and [§]Department of Chemistry, The Vanderbilt Institute of Nanoscale Science and Engineering, Vanderbilt University, Nashville, Tennessee 37235, United States

ABSTRACT Colloidal cadmium chalcogenide nanosheets with atomically precise thickness of a few atomic layers and size of 10−100 nm are two-dimensional (2D) quantum well materials with strong and precise quantum confinement in the thickness direction. Despite their many advantageous properties, excitons in these and other 2D metal chalcogenide materials are short-lived due to large radiative and nonradiative recombination rates, hindering their applications as light harvesting and charge separation/transport materials for solar energy conversion. We showed that these problems could be overcome in type-II CdSe/CdTe core/crown heteronanosheets (with CdTe crown laterally extending on the CdSe nanosheet core). Photoluminesence excitation measurement revealed that nearly all excitons generated in the CdSe and CdTe domains localized to the CdSe/CdTe interface to form long-lived charge transfer excitons (with electrons in the CdSe domain and hole in the CdTe domain). By ultrafast transient absorption spectroscopy, we showed that the efficient exciton localization efficiency could be attributed to ultrafast exciton localization (0.64 ± 0.07 ps), which was facilitated by large in-plane exciton mobility in these 2D materials and competed effectively with exiton trapping at the CdSe or CdTe domains. The spatial separation of electrons and holes across the CdSe/CdTe heterojunction effectively suppressed radiative and nonradiative recombination processes, leading to a long-lived charge transfer exciton state with a half-life of ∼41.7 ± 2.5 ns, ∼30 times longer than core-only CdSe nanosheets.

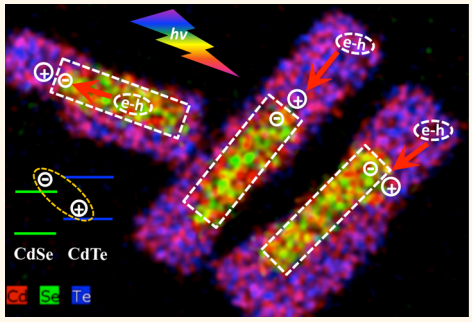

KEYWORDS: colloidal nanosheets · type-II heterostructures · charge separation · photocatalysis

Colloidal 2-D CdX (X = S, Se, Te) nanoplatelets (NPLs), or nanosheets (NSs), with atomically precise thickness of 1−2 nm have been reported recently.[1−6] The precise and strong quantum confinement in the thickness direction gives rise to uniform band edge positions and exciton energy across the NSs of tens to hundreds of nanometers in length and width. This enables rapid in-plane exciton and carrier motion, in addition to precise tuning of energetics (by thickness). Unfortunately, similar to other 2-dimensional (2D) materials (such as transition metal dichalcogenides[7,8]), strong electron−hole Coulomb interaction and large exposed surface lead to fast exciton radiative and nonradiative decay, respectively,[3] hindering their applications as light harvesting materials for solar energy conversion. It has been well demonstrated that in 0D quantum dots and 1D nanorods, type-II heterostructures (with conduction band minimum and valence band maximum residing in two different domains) can prolong exciton lifetime by increasing the spatial separation of the electron and hole.[9−23] Although several type-I heteronanosheets, such as CdSe/CdS or CdSe/CdZnS core/shell[24,25] and CdSe/CdS core/crown,[26,27] have been synthesized and studied, the preparation of type-II heteronanosheets has only been reported very recently.[28] This study demonstrates that excited state lifetime can also be extended in CdSe/CdTe core/crown type-II

* Address correspondence to tlian@emory.edu.

Received for review November 28, 2014 and accepted December 30, 2014.

Published online December 30, 2014
10.1021/nn506796m

heteronanosheets, similar to type-II quantum dots and nanorods. Previous studies of quasi-type-II CdSe/CdS dot-in-rod heteronanorods have shown that due to large electron−hole binding energy and presence of defects, ultrafast trapping of excitons on the CdS rod reduces the efficiency of exciton localization to the CdSe core.[29−32] Because similar trapping processes should also exist in type-II heteronanosheets, it is important to investigate how they may compete with the exciton localization process and whether the larger in-plane exciton mobility can reduce the effect of the undesirable exciton trapping pathways.[33]

In this paper, we report the first ultrafast spectroscopic study of exciton localization and interfacial separation process in CdSe/CdTe core/crown type-II nanosheets (with a CdTe NS crown laterally extending on a CdSe NS core, Scheme 1a). The structure was confirmed by electron microscopy, elemental analysis, and static and time-resolved optical spectroscopy. The formation of CdSe/CdTe type-II heterojunctions led to charge transfer (CT) absorption and emission features. Photoluminescence excitation measurements showed that excitons from CdTe and CdSe domains were localized to and separated across the CdSe/CdTe heterojunction to form CT excitons with near unity efficiency. The CT exciton formation process was shown to occur with a time constant of 0.64 ± 0.07 ps by transient absorption studies. The spatial separation of electrons and holes across the heterojunction reduced their radiative and noradiative recombination rates, leading to long-lived CT excitons with a half-life of 41.7 ± 2.5 ns, ~30 times longer than core-only CdSe NSs.

RESULTS AND DISCUSSIONS

Sample Preparation and Characterizations. CdSe NSs were synthesized according to literature procedures.[1−3] Lateral extension of CdTe on CdSe NSs was achieved following a reported synthetic procedures for CdTe NSs with a slight modification.[34] By injecting Te precursors at a lower rate and lower temperature than those reported for CdTe synthesis, CdTe heterogeneous nucleation on CdSe NSs can dominate over homogeneous nucleation in solution.[26,27] Detailed synthetic method and conditions can be found in the Methods section and Supporting Information (SI) and are similar to a recent independent report by Dubertret and co-workers.[28] Transmission electron microscopy (TEM) images of CdSe/CdTe nanosheets at different times after Te precursor injection (Figure 1a and S1) clearly showed a gradual increase of NS lateral dimension. The starting CdSe NSs (0 min) exhibited rectangular morphology with an average length and width of 28.0 (±2.5) nm × 7.0 (±1.0) nm, respectively. After 55 min of Te precursor injection, the NSs maintained their rectangular morphology but the average size increased to 71.0 (±7.7) nm × 21.3 (±3.7) nm, corresponding to ~8 fold increase in surface area.

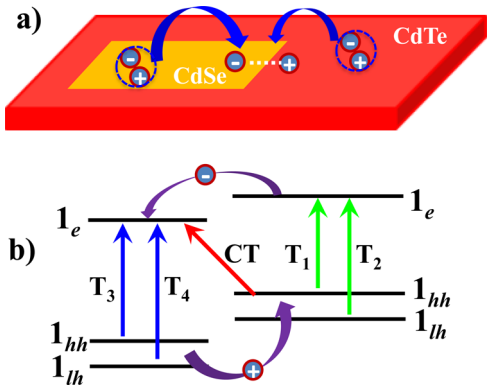

Scheme 1. (a) A schematic depiction of charge transfer exciton formation in Type-II CdSe/CdTe nanosheets. Photogenerated excitons in both CdSe and CdTe localize to the interface to form charge transfer excitons with electrons in CdSe and holes in CdTe. (b) Energy level diagram in Type-II CdSe/CdTe nanosheets. T1 (T3) and T2 (T4) are lowest energy heavy (1_{hh}) and light (1_{lh}) hole to electron (1_e) transitions, respectively, in CdTe (CdSe) and the charge transfer (CT) band corresponds to transition between heavy hole in CdTe and electron in CdSe. The charge separation processes are also indicated.

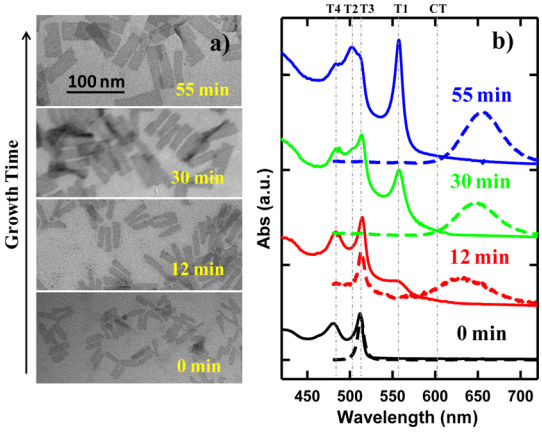

Figure 1. (a) TEM images and (b) absorption (solid line) and Photoluminescence (PL, dashed lines) spectra of CdSe/CdTe NSs at indicated growth times (starting with CdSe NSs at 0 min).

The absorption spectra (Figure 1b) showed three features that were consistent with the lateral extension of CdTe on CdSe. The exciton peak positions of NSs are determined by their thickness. The CdSe NS peaks, centered at ~512 nm (T3, n = 1 heavy hole to n = 1 electron, or $1_{hh}-1_e$[1]) and ~480 nm (T4, n = 1 light hole to n = 1 electron, or $1_{lh}-1_e$), remained unchanged during CdTe growth, indicating negligible change of CdSe thickness (~1.2 nm).[27] The amplitudes of two new peaks centered at ~556 nm (T1) and ~501 nm (T2) and a broad absorption tail from ~650 nm (CT) increased with growth time. The former (T1 and T2) matches the $1_{hh}-1_e$ and $1_{lh}-1_e$ transitions of CdTe NSs with a thickness of ~1.3 nm.[28,34] The CT band is energetically lower than both the lowest energy exciton transitions in CdSe (T3) and CdTe (T1) NSs and can be attributed to the charge transfer (CT) transition from the CdTe valence band (VB) edge to CdSe conduction band (CB)

edge (Scheme 1b), a characteristic feature of type-II heterostructures.[9] Photoluminescence (PL) spectra of these samples (Figure 1b, exciting at 400 nm) showed that upon CdTe growth, the PL of CdSe at ~512 nm was gradually replaced by CT emission centered at ~650 nm, showing negligible emission of CdTe NS (expected at ~556 nm).[34] These results confirm that the observed morphological changes are due to formation of CdSe/CdTe heteronanosheets instead of homogeneous nucleation of CdTe NS. In the following, we will focus on the 55 min sample for structural and spectroscopic characterizations.

High-angle annular dark-field (HAADF) scanning TEM (STEM) combined with energy-dispersive X-ray spectroscopy (EDX) was used to provide direct evidence for heterostructure formation. For the selected area in the HAADF image of Figure 2a, elemental maps for Cd, Se, and Te are shown in Figure 2c, d, and f, respectively. The Cd map matched well with TEM image; Se was only present in the center of nanosheets; and the Te map showed holes in the center, complementary to the Se map. The overlaid map, shown in Figure 2b, confirms that in these heterostructure, the CdTe NS laterally extends on CdSe seed, as illustrated in Scheme 1a.

Efficiency of Charge Transfer Exciton Formation. In Figure 3a, we compare the Photoluminescence Excitation (PLE, monitoring emission at 653 ± 1 nm) spectrum of CdSe/CdTe NSs with their absorptance spectrum. The latter represents the percentage of absorbed photons (*i.e.*, $1-10^{-OD}$, OD = optical density). By normalizing PLE and absorptance at the CT band, as done in Figure 3a, the ratios of these curves represent the relative emission QYs as a function of excitation wavelength (with QY at CT band excitation set to 1). As shown in Figure 3b, the relative QYs are near unity from 450 to 650 nm, indicating that all the photogenerated excitons can move to the CdSe/CdTe interface to form the CT excitons.

There are two implications from the near unity formation efficiency of the CT exciton. First, the exciton transport through CdTe and CdSe domains is fast enough to reach the CdSe/CdTe interface prior to their radiative and nonradiative decay. Second, the initial photogenerated excitons in both CdTe and CdSe domains can be dissociated across the CdSe/CdTe interface, in spite of the large exciton binding energy (~100s of meV) in these 2D nanosheets.[35,36] Similar processes have been observed in type-II single layer transition metal dichalcogenide heterojunctions[8,37] and can be explained by the fact that the energy required for exciton dissociation is compensated by the binding energy of the CT exciton.[8]

Ultrafast Charge Separation and Recombination Dynamics. The exciton localization and separation dynamics implied by the PLE result can be directly probed by transient absorption (TA) spectroscopy. In these measurements, we have used low excitation flux to ensure

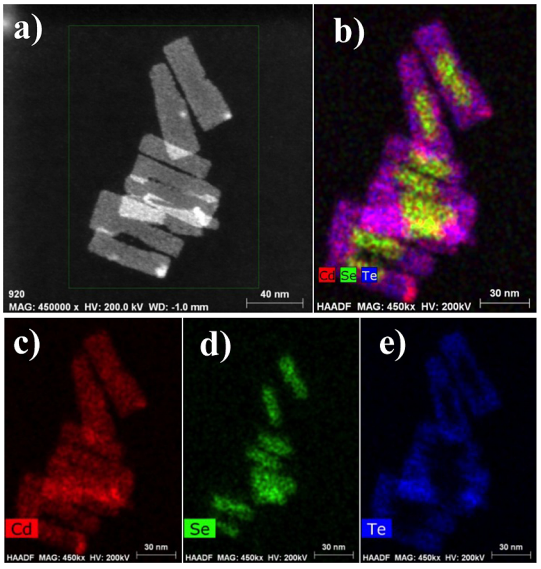

Figure 2. (a) HAADF STEM image of CdSe/CdTe nanosheet. (b) Overlaid elemental maps of Cd (red), Se (green), and Te (blue). Elemental maps of (c) Cd, (d) Se and (e) Te.

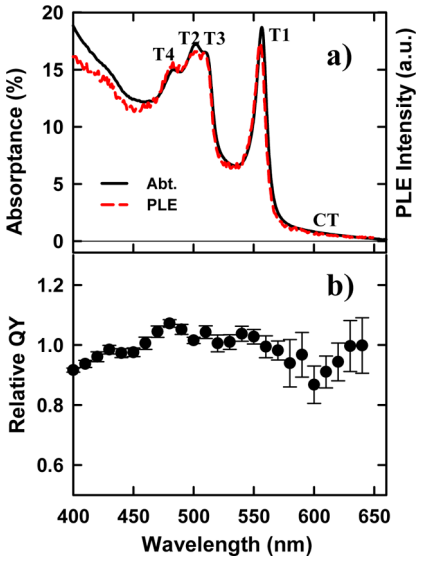

Figure 3. (a) Photoluminescence Excitation (PLE, red dashed line) and absorptance (Abt, black solid line) spectra of CdSe/CdTe NSs. These curves are normalized at the CT band. (b) Relative emission QYs (the ratio between absorptance and PLE) as a function of excitation wavelength. The relative QY was set to 1 at the CT band.

that the signal was dominated by single excitons (see Figure S3, SI for details), excluding the complications of multiexciton annihilation dynamics.[38,39] We first examined the CdSe/CdTe NSs with 625 nm excitation, where the CT band was selectively excited according to the absorption spectrum in Figure 1b. The resultant TA spectra and kinetics (Figure 4a and b) showed instantaneous bleach of T3 (~511 nm), T4 (~480 nm) and CT (~630 nm) bands and negligible subsequent changes of these TA features within the first nanosecond. Although part of the CT bleach was obscured

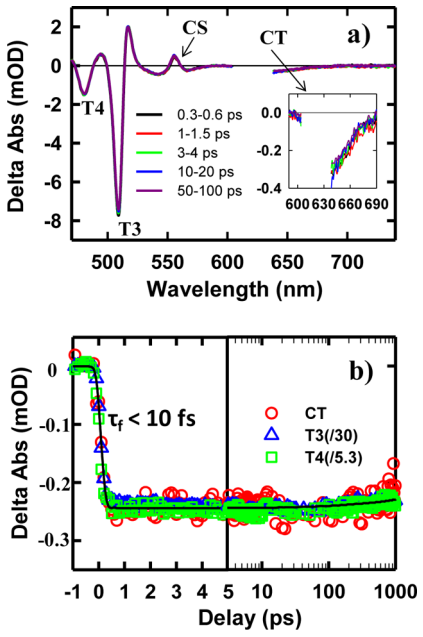

Figure 4. TA spectra of CdSe/CdTe heteronanosheets measured at 625 nm excitation of the CT band. (a) TA spectra at indicated delays (up to 100 ps). (b) Normalized comparison of TA kinetics of CT (red circles), T3 (blue triangles), and T4 (green squares) features and their fit (black solid line). The fit shows an instantaneous formation (<10 fs) and negligible decay in 1000 ps. The *x*-axis is in linear scale from −1 to 5 ps and logarithmic scale from 5 to 1000 ns.

by the scattered pump beam at 625 nm, it was fully observed with 400 nm excitation (see below). We have shown recently that the bleaches of exciton bands of CdSe NSs were caused by state-filling of the CB electron level,[40] similar to Cd chalcogenide quantum dots and nanorods.[41−44] The lack of hole filling induced exciton bleach is often attributed to the higher degeneracy of and stronger mixing between denser hole levels in the VB. Because CdTe and CdSe have similar band structure,[3] we expect that exciton bleach in CdTe nanosheets should also be dominated by state filling of CB levels. Therefore, the observed TA features indicate the direct generation of electrons in CdSe CB edge, consistent with the nature of the CT band (see Scheme 1b). The CT transition should also directly generate VB holes in CdTe. The presence of holes has been shown to shift the exciton peak position, giving rise to derivative like charge separated states (CS) features in TA spectrum.[20,40,43,45−48] Indeed, CS feature of T1 band was observed at 520−570 nm (see inset of Figure 4a and 5b). Therefore, these TA features confirm the proposed type-II electronic structure in Scheme 1.

We next investigated how the excitons generated at the CdTe crown can be localized to the CdSe/CdTe interface. In this experiment the CdSe/CdTe NSs were excited at 400 nm, where the CdSe and CdTe domains contributed to 16.8 and 83.2%, respectively, of the total

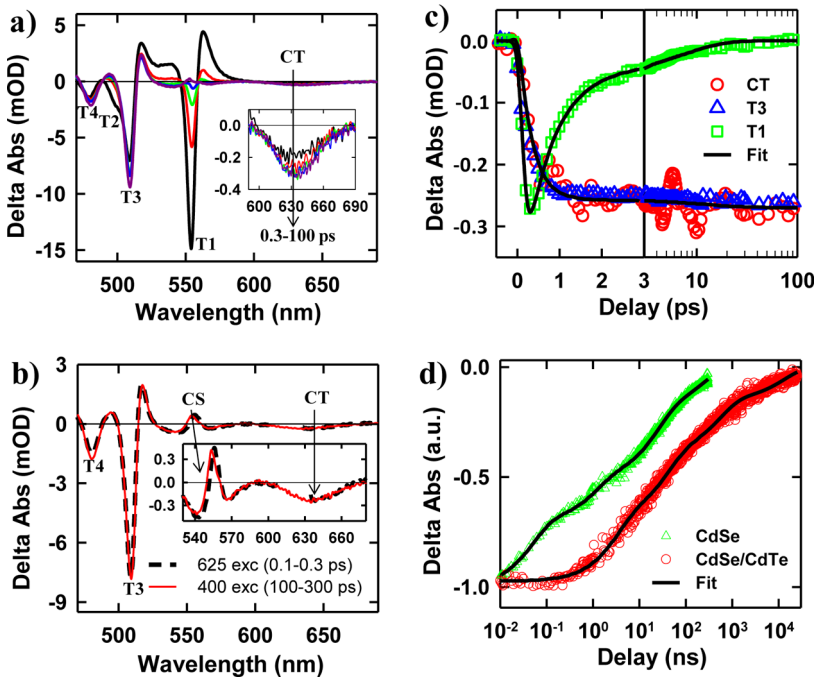

Figure 5. TA spectra and kinetics of CdSe/CdTe NSs. (a) TA spectra at 0.3−0.4 ps (black), 1−1.5 ps (red), 3−4 ps (green), 10−20 ps (blue), and 50−100 ps (purple) after 400 nm excitation. Inset: expanded view of the CT feature. (b) Comparison of TA spectra measured with 625 nm (at 0.1−0.3 ps, black dashed line) and 400 nm (at 100−300 ps, red solid line) excitation. Inset: expanded view of CS feature of T1 from 530 to 580 nm and CT band bleach from 590 to 690 nm. (c) TA kinetics of CT (610−650 nm, red circles), T3 (511 nm, blue triangles), and T1 (555 nm, green squares) in CdSe/CdTe NSs measured with 400 nm excitation and their multiexponential fits (black solid lines). (d) Comparison of electron lifetime (T3 exciton bleach recovery) in core-only CdSe (red circles) and CdSe/CdTe (green squares) NSs. The black solid lines are multiexponential fits.

absorption (Figure S4). The larger CdTe absorption is consistent with the ~7 fold larger surface area of CdTe than CdSe domain. The TA spectra (Figure 5a) showed ultrafast decay of T1 and T2 bleach and concomitant formation of the bleach of T3, T4 and the CT bands, consistent with electron transfer from CdTe to CdSe CB. After ~100 ps, T1 and T2 features completely disappeared and the resulting spectra were identical to the TA spectra measured with 625 nm excitation, as shown in Figure 5b, indicating complete conversion of excitons at CdSe and CdTe sheets to CT excitons across the CdTe/CdSe interface. This is consistent with the near unity CT band formation efficiency determined from the PLE measurement. Interestingly, the excitation wavelength independent final TA spectra in Figure 5b are in sharp contrast with previously examined CdSe/CdS heteronanorods, in which the competition of rapid exciton trapping on the CdS nanorod and localization to the CdSe core lead to excitation wavelength dependent branching ratio of long-lived exciton states.[29,30]

As shown in Figure 5c, the formation of CT and T3 bleach (electrons in CdSe 1_e level) and the recovery of T1 bleach (electrons in CdTe 1_e level) could be fitted with the same sets of parameters (Table S1, SI), confirming electron transfer from CdTe to CdSe. According to the fit, electron transfer kinetics from CdTe to CdSe was described as a biexponential process with time constants of 0.48 ± 0.09 ps (90.4 ± 0.4%) and 9.50 ± 0.85 ps (9.6 ± 0.3%). Electron transfer from CdTe to CdSe domains contains the contribution of exciton transport to the CdSe/CdTe interface and interfacial electron transfer across the heterojunction driven by the conduction band offset. A previous study on CdTe/CdSe core/shell QDs reported an electron transfer time of ~0.8 ps from CdTe to CdSe.[20] The main electron transfer component in our heteronanosheets is faster than the CdTe/CdSe core/shell QDs, which indicates that the intrananosheet exciton transport time is extremely fast, if not negligible, caused by the large in-plane exciton mobility. This observation is also consistent with our previous finding of ultrafast exciton quenching of CdSe NSs by decorated Pt nanoparticles.[40] In addition, the laterally extended 2D sheets might have smaller interfacial strain than curved core/shell QDs, which may reduce the possible interfacial charge transfer barrier.[49] The minor slow electron transfer component is likely caused by trapped excitons,[31,40,50] charge separation of which has to overcome the Coulomb potential barrier provided by the trapped holes.[50] 400 nm excitation should also generate excitons at CdSe core, which would separate at the interface by hole transfer to CdTe. This process should lead to derivative like features in the CdTe bands (Figure 4a and 5b). Unfortunately, the transient absorption signals at CdTe exciton bands were dominated by much larger state filling induced bleach and the smaller hole transfer induced change could not be independently probed. Furthermore, because of the spectral overlap of CdSe with CdTe transitions, selective excitation of the CdSe sheet was not experimentally feasible.

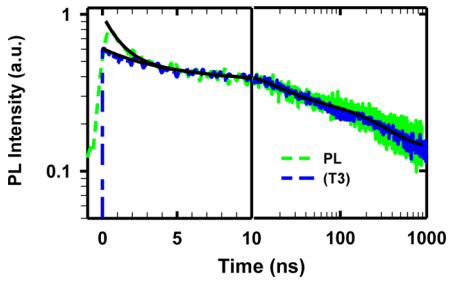

Figure 6. Comparison of time-resolved PL decay (green dashed line) and TA T3 (CT) bleach recovery kinetics of (blue dashed line) in CdSe/CdTe type-II NSs measured with 400 nm excitation. The black solid lines are multiexponential fits and fitting parameters are listed in Table S2.

The electrons in the CT states were long-lived, as indicated by the long-lived T3 bleach on the 1 ns to 20 μs time scale (Figure S6). The kinetics of T3 recovery (Figure 5d) was fitted by multiexponential decay with a half-life of 41.7 ± 2.5 ns. The fitting parameters were listed in Table S1. As a comparison, the TA spectra of core-only CdSe NSs was also measured (Figure S7). The T3 exciton bleach kinetics of CdSe (Figure 5d) showed a half-life of 1.4 ± 0.2 ns. Therefore, the CB electron lifetime was prolonged by ~30-fold in type-II NSs. Because T3 exciton bleach only reflected the CB electron population, we turned to PL decay (depending on both CB electrons and VB holes) to probe the effect of CT exciton formation on VB holes. The time-resolved PL decay and T3 exciton bleach kinetics of CdSe/CdTe NSs were compared in Figure 6. The PL decay matched well with the T3 bleach recovery between 5−1000 ns, confirming that the spatial separation of electrons and holes across the CdTe/CdSe interface gave rise to long-lived CT excitons. This is consistent with a recent report by Dubertret and co-workers.[28] Interestingly, the PL decay showed a fast component (with 50.2 ± 1.7% amplitude and a time constant of 1.2 ± 0.1 ns, Table S2) that was not present in the T3 bleach recovery, which can only be assigned to the trapping of VB holes in the CdTe domain. Hole trapping on similar time scales has been identified in CdSe and CdSe/CdS nanosheets.[50] Because this hole trapping process does not lead to the decay of the CB electron, it indicates that the spatial separation of electrons and holes across the heterojunction also slows down their nonradiative recombination at trapped sites.

It should be noted that similar efficient exciton localization was observed in type-I CdSe/CdS core/crown nanosheets.[27] These efficient in-plane exciton transports are in contrast to 1-D CdSe/CdS NR heterostructures, in which the localization efficiency is significantly less than unity due to hole-trap induced exciton trapping on the CdS rod.[29,30] We tentatively

attribute the efficient exciton localization in NSs to large exciton and carrier mobility in these atomically flat materials. It has been proposed that the exciton center-of-mass wave function may be delocalized throughout the entire NS,[39] which can also lead to efficient exciton localization in our CdSe/CdTe NSs. It is also interesting to compare the CdSe/CdTe heterostructure to MoS_2/WS_2 van der Waals heterostructures at which a ~50 fs hole transfer time was reported.[8] Although the covalent/ionic bonding at our CdSe/CdTe interface is much stronger than van der Waals interactions per unit area,[8] the smaller total interfacial area in the core/crown structure than the stacked structure might lead to weaker total electronic coupling and therefore slower charge separation. Nonetheless, the charge separation rate in these CdSe/CdTe core/crown heterostructure is still much faster than excited state lifetime of NSs (on the order of ns[51]), which gives rise to unity yield for forming the long-lived CT exciton states. Finally, the efficient exciton localization in CdSe/CdTe nanosheets may offer a new class of materials for constructing triadic nanosheet heterostructures (such as CdSe/CdTe/Pt) for light-driven H_2 generation. Our recent study suggests that in CdSe NS-Pt heterostructures, the ultrafast exciton mobility leads to efficient quenching of excitons by energy transfer, which limits the utility of such structure in solar-driven H_2 generation.[40] The ability to form long-lived charge transfer excitons at CdSe/CdTe interface may allow efficient electron transfer to Pt in CdSe/CdTe/Pt triadic structures.

CONCLUSIONS

In conclusion, we have studied the ultrafast exciton dynamics in colloidal type-II CdSe/CdTe core/crown heteronanosheets. The formation of the heterostructure was confirmed by absorption, emission, electron microscopy and element analysis. By PLE measurements, we showed that excitons generated in CdSe and CdTe domains could be localized to the CdSe/CdTe heterojunction to form charge transfer excitons with unity efficiency. Using transient absorption spectroscopy, we showed that these charge transfer excitons were formed on the ultrafast time scale (half-life ~0.64 ± 0.07 ps) due to facile in-plane exciton motion and interfacial electron transfer. The spatial separation of electrons and holes at the CT states effectively suppressed radiative and nonradiative recombination, leading to long-lived charge transfer exciton state (half-life ~41.7 ± 2.5 ns). Therefore, these 2D type-II heteronanosheets are promising materials for efficient light harvesting and charge separation and transport in solar energy conversion applications.

METHODS

CdSe Nanosheets (NSs) were synthesized following procedures reported in the literature, with slight modifications.[1−3] CdTe extension on CdSe NSs were achieved by injection Te precursors into a flask containing Cd precursors and CdSe NSs. Aliquots of colloidal solution were taken out using a syringe to monitor the CdTe crown growth. Details can be found in the Supporting Information.

Instruments for structural and optical characterization of the NSs were also described in the SI. Both femtoseconds and nanoseconds transient absorption (TA) measurements were based on a regeneratively amplified Ti:sapphire laser system (Coherent Legend, 800 nm, 150 fs, 2.4 mJ/pulse, and 1 kHz repetition rate). The fs and ns TA signals were detected and analyzed by Helios and EOS spectrometers (Ultrafast Systems LLC), respectively.

Conflict of Interest: The authors declare no competing financial interest.

Acknowledgment. We gratefully acknowledge the financial support from the National Science Foundation (CHE-1309817). J.R.M. acknowledges funding by the National Science Foundation (CHE-1213758). STEM and EDS images were acquired using an FEI Tecnai Osiris electron microscope supported by the National Science Foundation (EPS-1004083). We also thank Jacob Olshansky and Fadekemi Oba from University of California, Berkeley for their assistance in TEM measurements.

Supporting Information Available: Sample synthesis, TEM images, transient absorption apparatus, additional TA spectra, kinetics fitting. This material is available free of charge *via* the Internet at http://pubs.acs.org.

REFERENCES AND NOTES

1. Ithurria, S.; Dubertret, B. Quasi 2D Colloidal CdSe Platelets with Thicknesses Controlled at the Atomic Level. *J. Am. Chem. Soc.* **2008**, *130*, 16504–16505.
2. Ithurria, S.; Bousquet, G.; Dubertret, B. Continuous Transition from 3D to 1D Confinement Observed during the Formation of CdSe Nanoplatelets. *J. Am. Chem. Soc.* **2011**, *133*, 3070–3077.
3. Ithurria, S.; Tessier, M. D.; Mahler, B.; Lobo, R. P. S. M.; Dubertret, B.; Efros, A. L. Colloidal Nanoplatelets with Two-Dimensional Electronic Structure. *Nat. Mater.* **2011**, *10*, 936–941.
4. Joo, J.; Son, J. S.; Kwon, S. G.; Yu, J. H.; Hyeon, T. Low-Temperature Solution-Phase Synthesis of Quantum Well Structured CdSe Nanoribbons. *J. Am. Chem. Soc.* **2006**, *128*, 5632–5633.
5. Son, J. S.; Wen, X.-D.; Joo, J.; Chae, J.; Baek, S.-i.; Park, K.; Kim, J. H.; An, K.; Yu, J. H.; Kwon, S. G.; *et al.* Large-Scale Soft Colloidal Template Synthesis of 1.4 nm Thick CdSe Nanosheets. *Angew. Chem., Int. Ed.* **2009**, *48*, 6861–6864.
6. Son, J. S.; Yu, J. H.; Kwon, S. G.; Lee, J.; Joo, J.; Hyeon, T. Colloidal Synthesis of Ultrathin Two-Dimensional Semiconductor Nanocrystals. *Adv. Mater.* **2011**, *23*, 3214–3219.
7. Geim, A. K.; Grigorieva, I. V. Van der Waals heterostructures. *Nature* **2013**, *499*, 419–425.
8. Hong, X.; Kim, J.; Shi, S.-F.; Zhang, Y.; Jin, C.; Sun, Y.; Tongay, S.; Wu, J.; Zhang, Y.; Wang, F. Ultrafast charge transfer in atomically thin MoS2/WS2 heterostructures. *Nat. Nanotechnol.* **2014**, *9*, 682–686.
9. Kim, S.; Fisher, B.; Eisler, H.-J.; Bawendi, M. Type-II Quantum Dots: CdTe/CdSe(Core/Shell) and CdSe/ZnTe(Core/Shell) Heterostructures. *J. Am. Chem. Soc.* **2003**, *125*, 11466–11467.
10. Halpert, J. E.; Porter, V. J.; Zimmer, J. P.; Bawendi, M. G. Synthesis of CdSe/CdTe Nanobarbells. *J. Am. Chem. Soc.* **2006**, *128*, 12590–12591.
11. Kumar, S.; Jones, M.; Lo, S. S.; Scholes, G. D. Nanorod Heterostructures Showing Photoinduced Charge Separation. *Small* **2007**, *3*, 1633–1639.
12. Zhong, H. Z.; Scholes, G. D. Shape Tuning of Type II CdTe-CdSe Colloidal Nanocrystal Heterostructures through Seeded Growth. *J. Am. Chem. Soc.* **2009**, *131*, 9170–9071.

13. Kirsanova, M.; Nemchinov, A.; Hewa-Kasakarage, N. N.; Schmall, N.; Zamkov, M. Synthesis of ZnSe/CdS/ZnSe Nanobarbells Showing Photoinduced Charge Separation. *Chem. Mater.* **2009**, *21*, 4305–4309.
14. Dorfs, D.; Salant, A.; Popov, I.; Banin, U. ZnSe Quantum Dots Within CdS Nanorods: A Seeded-Growth Type-II System. *Small* **2008**, *4*, 1319–1323.
15. Balet, L. P.; Ivanov, S. A.; Piryatinski, A.; Achermann, M.; Klimov, V. I. Inverted Core/Shell Nanocrystals Continuously Tunable between Type-I and Type-II Localization Regimes. *Nano Lett.* **2004**, *4*, 1485–1488.
16. Milliron, D. J.; Hughes, S. M.; Cui, Y.; Manna, L.; Li, J.; Wang, L.-W.; Paul Alivisatos, A. Colloidal Nanocrystal Heterostructures With Linear and Branched Topology. *Nature* **2004**, *430*, 190–195.
17. Peng, P.; Milliron, D. J.; Hughes, S. M.; Johnson, J. C.; Alivisatos, A. P.; Saykally, R. J. Femtosecond Spectroscopy of Carrier Relaxation Dynamics in Type II CdSe/CdTe Tetrapod Heteronanostructures. *Nano Lett.* **2005**, *5*, 1809–1813.
18. Jones, M.; Kumar, S.; Lo, S. S.; Scholes, G. D. Exciton Trapping and Recombination in Type II CdSe/CdTe Nanorod Heterostructures. *J. Phys. Chem. C* **2008**, *112*, 5423–5431.
19. Hewa-Kasakarage, N. N.; El-Khoury, P. Z.; Tarnovsky, A. N.; Kirsanova, M.; Nemitz, I.; Nemchinov, A.; Zamkov, M. Ultrafast Carrier Dynamics in Type II ZnSe/CdS/ZnSe Nanobarbells. *ACS Nano* **2010**, *4*, 1837–1844.
20. Zhu, H.; Song, N.; Lian, T. Wave Function Engineering for Ultrafast Charge Separation and Slow Charge Recombination in Type II Core/Shell Quantum Dots. *J. Am. Chem. Soc.* **2011**, *133*, 8762–8771.
21. Jin, S.; Zhang, J.; Schaller, R. D.; Rajh, T.; Wiederrecht, G. P. Ultrafast Charge Separation from Highly Reductive ZnTe/CdSe Type II Quantum Dots. *J. Phys. Chem. Lett.* **2012**, *3*, 2052–2058.
22. Ivanov, S. A.; Piryatinski, A.; Nanda, J.; Tretiak, S.; Zavadil, K. R.; Wallace, W. O.; Werder, D.; Klimov, V. I. Type-II Core/Shell CdS/ZnSe Nanocrystals: Synthesis, Electronic Structures, And Spectroscopic Properties. *J. Am. Chem. Soc.* **2007**, *129*, 11708–11719.
23. Zhu, H.; Chen, Z.; Wu, K.; Lian, T. Wavelength Dependent Efficient Photoreduction of Redox Mediators Using Type II ZnSe/CdS Nanorod Heterostructures. *Chem. Sci.* **2014**, *5*, 3905–3914.
24. Mahler, B.; Nadal, B.; Bouet, C.; Patriarche, G.; Dubertret, B. Core/Shell Colloidal Semiconductor Nanoplatelets. *J. Am. Chem. Soc.* **2012**, *134*, 18591–18598.
25. Ithurria, S.; Talapin, D. V. Colloidal Atomic Layer Deposition (c-ALD) using Self-Limiting Reactions at Nanocrystal Surface Coupled to Phase Transfer between Polar and Nonpolar Media. *J. Am. Chem. Soc.* **2012**, *134*, 18585–18590.
26. Prudnikau, A.; Chuvilin, A.; Artemyev, M. CdSe−CdS Nanoheteroplatelets with Efficient Photoexcitation of Central CdSe Region through Epitaxially Grown CdS Wings. *J. Am. Chem. Soc.* **2013**, *135*, 14476–14479.
27. Tessier, M. D.; Spinicelli, P.; Dupont, D.; Patriarche, G.; Ithurria, S.; Dubertret, B. Efficient Exciton Concentrators Built from Colloidal Core/Crown CdSe/CdS Semiconductor Nanoplatelets. *Nano Lett.* **2013**, *14*, 207–213.
28. Pedetti, S.; Ithurria, S.; Heuclin, H.; Patriarche, G.; Dubertret, B. Type-II CdSe/CdTe Core/Crown Semiconductor Nanoplatelets. *J. Am. Chem. Soc.* **2014**, *136*, 16430–16438.
29. Wu, K.; Rodríguez-Córdoba, W. E.; Liu, Z.; Zhu, H.; Lian, T. Beyond Band Alignment: Hole Localization Driven Formation of Three Spatially Separated Long-Lived Exciton States in CdSe/CdS Nanorods. *ACS Nano* **2013**, *7*, 7173–7185.
30. She, C.; Bryant, G. W.; Demortière, A.; Shevchenko, E. V.; Pelton, M. Controlling the Spatial Location of Photoexcited Electrons in Semiconductor CdSe/CdS Core/Shell Nanorods. *Phys. Rev. B: Condens. Matter Mater. Phys.* **2013**, *87*, 155427.
31. Mauser, C.; Da Como, E.; Baldauf, J.; Rogach, A. L.; Huang, J.; Talapin, D. V.; Feldmann, J. Spatio-temporal Dynamics of Coupled Electrons and Holes in Nanosize CdSe-CdS Semiconductor Tetrapods. *Phys. Rev. B: Condens. Matter Mater. Phys.* **2010**, *82*, 081306.
32. Kunneman, L. T.; Zanella, M.; Manna, L.; Siebbeles, L. D. A.; Schins, J. M. Mobility and Spatial Distribution of Photoexcited Electrons in CdSe/CdS Nanorods. *J. Phys. Chem. C* **2013**, *117*, 3146–3151.
33. Coleman, J. N.; Lotya, M.; O'Neill, A.; Bergin, S. D.; King, P. J.; Khan, U.; Young, K.; Gaucher, A.; De, S.; Smith, R. J.; *et al.* Two-Dimensional Nanosheets Produced by Liquid Exfoliation of Layered Materials. *Science* **2011**, *331*, 568–571.
34. Pedetti, S.; Nadal, B.; Lhuillier, E.; Mahler, B.; Bouet, C.; Abécassis, B.; Xu, X.; Dubertret, B. Optimized Synthesis of CdTe Nanoplatelets and Photoresponse of CdTe Nanoplatelets Films. *Chem. Mater.* **2013**, *25*, 2455–2462.
35. Grim, J. Q.; Christodoulou, S.; Di Stasio, F.; Krahne, R.; Cingolani, R.; Manna, L.; Moreels, I. Continuous-Wave Biexciton Lasing at Room Temperature Using Solution-Processed Quantum Wells. *Nat. Nanotechnol.* **2014**, *9*, 891–895.
36. Benchamekh, R.; Gippius, N. A.; Even, J.; Nestoklon, M. O.; Jancu, J. M.; Ithurria, S.; Dubertret, B.; Efros, A. L.; Voisin, P. Tight-Binding Calculations of Image-Charge Effects in Colloidal Nanoscale Platelets of CdSe. *Phys. Rev. B: Condens. Matter Mater. Phys.* **2014**, *89*, 035307.
37. Ceballos, F.; Bellus, M. Z.; Chiu, H.-Y.; Zhao, H. Ultrafast Charge Separation and Indirect Exciton Formation in a MoS2-MoSe2 van der Waals Heterostructure. *ACS Nano* **2014**, 10.1021/nn505736z.
38. Pelton, M.; Ithurria, S.; Schaller, R. D.; Dolzhnikov, D. S.; Talapin, D. V. Carrier Cooling in Colloidal Quantum Wells. *Nano Lett.* **2012**, *12*, 6158–6163.
39. Kunneman, L. T.; Tessier, M. D.; Heuclin, H.; Dubertret, B.; Aulin, Y. V.; Grozema, F. C.; Schins, J. M.; Siebbeles, L. D. A. Bimolecular Auger Recombination of Electron−Hole Pairs in Two-Dimensional CdSe and CdSe/CdZnS Core/Shell Nanoplatelets. *J. Phys. Chem. Lett.* **2013**, *4*, 3574–3578.
40. Wu, K.; Li, Q.; Du, y.; Chen, Z.; Lian, T. Ultrafast Exciton Quenching by Energy and Electron Transfer in Colloidal CdSe Nanosheet-Pt Heterostructures. *Chem. Sci.* **2014**, 10.1039/C4SC02994A.
41. Klimov, V. I. Optical Nonlinearities and Ultrafast Carrier Dynamics in Semiconductor Nanocrystals. *J. Phys. Chem. B* **2000**, *104*, 6112–6123.
42. Zhu, H.; Lian, T. Enhanced Multiple Exciton Dissociation from CdSe Quantum Rods: The Effect of Nanocrystal Shape. *J. Am. Chem. Soc.* **2012**, *134*, 11289–11297.
43. Wu, K.; Zhu, H.; Liu, Z.; Rodríguez-Córdoba, W.; Lian, T. Ultrafast Charge Separation and Long-Lived Charge Separated State in Photocatalytic CdS−Pt Nanorod Heterostructures. *J. Am. Chem. Soc.* **2012**, *134*, 10337–10340.
44. Huang, J.; Stockwell, D.; Huang, Z. Q.; Mohler, D. L.; Lian, T. Q. Photoinduced Ultrafast Electron Transfer from CdSe Quantum Dots to Re-bipyridyl Complexes. *J. Am. Chem. Soc.* **2008**, *130*, 5632–5633.
45. Wu, K.; Chen, Z.; Lv, H.; Zhu, H.; Hill, C. L.; Lian, T. Hole Removal Rate Limits Photo-driven H2 Generation Efficiency in CdS-Pt and CdSe/CdS-Pt Semiconductor Nanorod-Metal Tip Heterostructures. *J. Am. Chem. Soc.* **2014**, *136*, 7708–7716.
46. Wu, K.; Song, N.; Liu, Z.; Zhu, H.; Rodríguez-Córdoba, W.; Lian, T. Interfacial Charge Separation and Recombination in InP and Quasi-Type II InP/CdS Core/Shell Quantum Dot-Molecular Acceptor Complexes. *J. Phys. Chem. A* **2013**, *117*, 7561–7570.
47. Wu, K.; Liu, Z.; Zhu, H.; Lian, T. Exciton Annihilation and Dissociation Dynamics in Group II−V Cd3P2 Quantum Dots. *J. Phys. Chem. A* **2013**, *117*, 6362–6372.
48. Zhu, H. M.; Song, N. H.; Lian, T. Q. Controlling Charge Separation and Recombination Rates in CdSe/ZnS Type I Core-Shell Quantum Dots by Shell Thicknesses. *J. Am. Chem. Soc.* **2010**, *132*, 15038–15045.
49. Smith, A. M.; Nie, S. Semiconductor Nanocrystals: Structure, Properties, and Band Gap Engineering. *Acc. Chem. Res.* **2009**, *43*, 190–200.

50. Kunneman, L. T.; Schins, J. M.; Pedetti, S.; Heuclin, H.; Grozema, F. C.; Houtepen, A. J.; Dubertret, B.; Siebbeles, L. D. A. Nature and Decay Pathways of Photoexcited States in CdSe and CdSe/CdS Nanoplatelets. *Nano Lett.* **2014**, *14*, 7039–7045.
51. Biadala, L.; Liu, F.; Tessier, M. D.; Yakovlev, D. R.; Dubertret, B.; Bayer, M. Recombination Dynamics of Band Edge Excitons in Quasi-Two-Dimensional CdSe Nanoplatelets. *Nano Lett.* **2014**, *14*, 1134–1139.